Nonresonant femtosecond laser vaporization of aqueous protein preserves folded structure

John J. Brady, Elizabeth J. Judge, and Robert J. Levis[1]

Center for Advanced Photonics, Department of Chemistry, Temple University, 1901 North 13th Street, Philadelphia, PA 19122

Edited by Margaret M. Murnane, University of Colorado at Boulder, Boulder, CO, and approved June 13, 2011 (received for review April 8, 2011)

Femtosecond laser vaporization-based mass spectrometry can be used to measure protein conformation in vitro at atmospheric pressure. Cytochrome c and lysozyme are vaporized from the condensed phase into the gas phase intact when exposed to an intense (10^{13} W/cm^2), nonresonant (800 nm), ultrafast (75 fs) laser pulse. Electrospray postionization time-of-flight mass spectrometry reveals that the vaporized protein maintains the solution-phase conformation through measurement of the charge-state distribution and the collision-induced dissociation channels.

multiphoton | nonthermal

The interaction of intense, ultrashort laser pulses with matter has resulted in a number of remarkable unique phenomena including above threshold ionization (1, 2), high harmonic generation (3–5), Coulomb explosion (6), nonadiabatic excitation of polyatomic molecules (7, 8), neutron emission from clusters (9, 10), and the creation of attosecond laser pulses (5). Intense laser-matter interactions are currently used to determine polyatomic molecular electronic structure (11) and nuclear dynamics (12). Biomolecular structure determination represents a unique frontier for ultraintense laser experiments. In this regard, methods to deliver nonvolatile biological molecules intact into the gas phase, preferably maintaining condensed phase structure, are of interest. We recently reported that intense, nonresonant, ultrafast laser pulses could be used to deliver proteins with molecular weights up to 45 kDa into the gas phase without fragmentation (13). One motivation for this investigation is that for femtosecond laser vaporization to be of value for protein structural determination, the vaporization must ideally preserve the condensed phase primary, secondary, and tertiary conformation. Another motivation is the fact that the analysis of biological structure in situ presents a significant challenge. As a first step toward this goal, we investigate the conformation of proteins vaporized from the solution phase, in vitro, using intense, nonresonant femtosecond laser pulses.

The biological function of a protein is determined by both primary sequence and structural conformation, with the latter governed by inter- and intramolecular covalent and noncovalent interactions. Techniques such as X-ray crystallography (14), NMR spectroscopy (15), and hydroxyl-radical protein footprinting (16) are commonly used to determine protein conformation and to probe noncovalent interactions. Another emerging method, electrospray ionization mass spectrometry (ESI-MS) (17) can be used to assess protein conformation in the electrospray solvent solution because folded protein typically displays one or two intense peaks in the mass spectrum (18). Protein in an unfolded conformation results in a bell-shaped distribution of the peaks with the centroid of the distribution occurring at a lower m/z value (than the folded features) due to the basic amino acids being revealed and protonated (18). Changes in temperature, solvent, pH, and salt concentration will alter the equilibrium concentration of folded and unfolded protein and thus alter the observed mass spectrum. Although remarkably successful, the aforementioned methods are not amenable for ex vivo studies of protein conformation and require extensive sample manipulation prior to measurement. For example, the extraction and preparation steps typically result in denaturing conditions, altering the equilibrium concentration of folded/unfolded protein. Therefore, a key question concerns whether protein can be transferred from the condensed phase into the gas phase without altering the structural conformation.

Nanosecond laser-based methods provide the opportunity to directly sample condensed phase material, but requires the addition of a matrix to transfer analyte into the gas phase. For example, matrix-assisted laser desorption/ionization (MALDI) has been used for ex vivo spatial distribution analysis of protein (19). In MALDI, the nanosecond laser pulse couples into the externally applied matrix through a one-photon resonant excitation process at a laser intensity of approximately 10^6 to 10^7 W/cm^2. The absorbed energy is transferred from the matrix to the condensed phase allowing for desorption and ionization of both the matrix and protein (20). Although MALDI-MS has successfully analyzed a variety of molecules there is no provision for directly obtaining structural information for a protein. Such information requires extensive sample manipulation (21–23).

The coupling of laser-based desorption with electrospray postionization can allow not only for identification but also structural information for a given protein. Electrospray postionization of laser desorbed proteins has been achieved using techniques such as laser ablation electrospray ionization (24), electrospray-assisted laser desorption ionization (25), and matrix-assisted laser desorption electrospray ionization (26, 27). The aqueous proteins are delivered into the gas phase at atmospheric pressure using a nanosecond laser resonant with a vibrational transition in water. The deposition of energy into the water induces a phase explosion similar to MALDI, transferring material into the gas phase (24). The accompanying heating in the nanosecond laser desorption event presumably causes the aqueous protein to unfold. For example, unfolded bovine cytochrome c is observed in the mass spectrum upon infrared nanosecond laser desorption with electrospray postionization (25–28).

The use of nonresonant femtosecond laser pulses for vaporization may prevent thermal processes because the energy of the laser pulse is deposited into the system on a timescale much faster than that required for any ensuing thermal response. Time-resolved measurements in metallic systems reveal that after the initial electronic excitation, the internal modes of the condensed phase system heat on the picosecond to nanosecond timescale (29). If the nonequilbrium channel of vaporization occurs prior to thermalization to protein modes, dissociation can be avoided. In fact, the interaction of intense, nonresonant, femtosecond laser pulses (70 fs, 10^{13} W/cm^2) with a condensed phase sample at atmospheric pressure results in the intact vaporization of a wide variety of nonvolatile polyatomic molecules in systems ranging from explosive formulations to plant tissue (30–33). The discovery that a strong field femtosecond laser pulse can transfer neu-

Author contributions: J.J.B., E.J.J., and R.J.L. designed research; J.J.B., E.J.J., and R.J.L. performed research; J.J.B. and E.J.J. analyzed data; and J.J.B., E.J.J., and R.J.L. wrote the paper.

The authors declare no conflict of interest.

This article is a PNAS Direct Submission.

[1]To whom correspondence should be addressed. E-mail: rjlevis@temple.edu.

tral macromolecules into the gas phase intact (34) was unanticipated because isolated molecules in vacuum exposed to an intense laser pulse will ionize and possibly fragment (35, 36). The nonresonant femtosecond laser pulse can, in principle, couple into and vaporize all molecules in a given sample. This nonlinear excitation implies that the sample preparation steps of elution and mixing with a matrix are not necessary. Direct analysis of molecules ranging in size from pharmaceuticals (~300 Da) to proteins (>40 kDa) has been performed using the laser electrospray mass spectrometry (LEMS) method (13, 30–34) where ionization, mass analysis, and detection of the femtosecond laser-vaporized sample is achieved via atmospheric pressure ESI-TOF-MS.

In this work, we investigate the interaction of intense nonresonant femtosecond laser pulses with aqueous proteins to determine whether nonequilibrium processes enable the transfer of protein into the gas phase without altering the initial condensed phase structural conformation. The conformation of the vaporized protein is probed by measuring the resulting electrospray postionization mass spectrometry charge-state distribution as well as the collision-induced dissociation (CID) channels. The LEMS measurements, as a function of electrospray solvent pH and sample pH, are compared to conventional ESI-MS experiments.

Results

Conventional ESI-MS and LEMS of Aqueous Cytochrome c. The charge-state distributions measured after conventional ESI-MS are shown as a function of the electrospray solvent pH in Fig. 1 *A–D*. The ESI mass spectrum of cytochrome c electrosprayed from a solvent at pH 7.18 displays two distributions: one containing predominantly the 8 and 7+ charge states and the second containing a bell-shaped distribution (ranging from 17 to 9+) centered at the 12+ charge state (Fig. 1*A*). The n+ charge state represents the ion with m/z $(M + n)/(n)$, where M is the mass of the molecule and n is the number of additional protons (H^+) bound to the molecule. As the pH of the electrospray solvent is decreased to a pH of 4.06, the fraction of signal in the bell-shaped distribution centered at the 12+ charge state increases (Fig. 1*D*).

The charge-state distributions measured after femtosecond laser vaporization with electrospray postionization are shown as a function of the electrospray solvent pH in Fig. 1 *E–H*. Only the 8 and 7+ charge states are detected when the vaporized protein was captured and ionized by an electrospray plume at pH 7.18 (Fig. 1*E*) or 6.07 (Fig. 1*F*). The charge-state distribution centered at 12+ is detected in the mass spectrum when the vaporized protein is captured by an electrospray plume at pH 5.06 (Fig. 1*G*) or 4.06 (Fig. 1*H*). The LEMS mass spectrum as a function of the pH of the aqueous cytochrome c solution is shown in Fig. 2. The electrospray solvent for this experiment was maintained at a pH of 7.06. The mass spectrum for protein vaporized from a sample solution at pH 7 displays a high abundance peak at the 7+ charge state with low abundance peaks at 8, 6, 5, and 4+ charge states (Fig. 2*A*). The LEMS analysis for vaporization from a protein solution at a pH of approximately 3 reveals the 7+ charge state and a bell-shaped distribution ranging from 17 to 9+ centered at 12+ (Fig. 2*B*).

CID Conventional ESI-MS and LEMS of Aqueous Lysozyme. Collision-induced dissociation of the vaporized molecules can be performed by increasing the voltage difference (acceleration potential) between the capillary exit and the skimmer in the ESI source. At a low acceleration potential, no dissociation occurs due to the low collision energy with the background gas. As the acceleration potential approaches 400 V, the energy transferred into the analyte upon a collision with background gas increases, enabling dissociation. The conventional ESI mass spectra of lysozyme at acceleration potentials ranging from 50 to 390 V are shown in Fig. 3*A*. The mass spectrum acquired at an acceleration potential of 50 V reveals a bell-shaped distribution corresponding to the charge states 13 to 8+. The bell-shaped distribution is maintained with increasing collision energy, but shifts to lower charge states as the acceleration potential approaches 390 V. The integrated ion signal intensity of lysozyme as a function of acceleration potential using conventional ESI-MS is shown in Fig. 3*C*.

The LEMS mass spectrum for lysozyme collected at acceleration potential of 100 V displays only the 10 and 9+ charge states (Fig. 3*B*). Increasing the acceleration potential to 390 V, results in an increase in the ion abundance with no additional fragmentation or change in the charge-state distribution. The integrated ion signal intensity of lysozyme as a function of acceleration potential using LEMS is shown in Fig. 3*D*.

Discussion

Analysis of the Conventional ESI and LEMS Mass Spectra of Aqueous Cytochrome c. The ESI mass spectrum of aqueous cytochrome c, measured as a function of acid concentration, serves as a calibration for the analysis of protein structure after laser vaporization and electrospray postionization (Fig. 1 *A–D*). When cytochrome c was electrosprayed from a solution at pH 7, the 8 and 7+ charge states were observed. The 8 and 7+ charge states correspond to a folded conformation of cytochrome c as revealed by nano-ESI-MS experiments (37), and each charge state may contain several different conformations of the three-dimensional protein structure (38). In addition to the folded protein, a bell-shaped distribution centered at the 12+ charge state, corresponding to

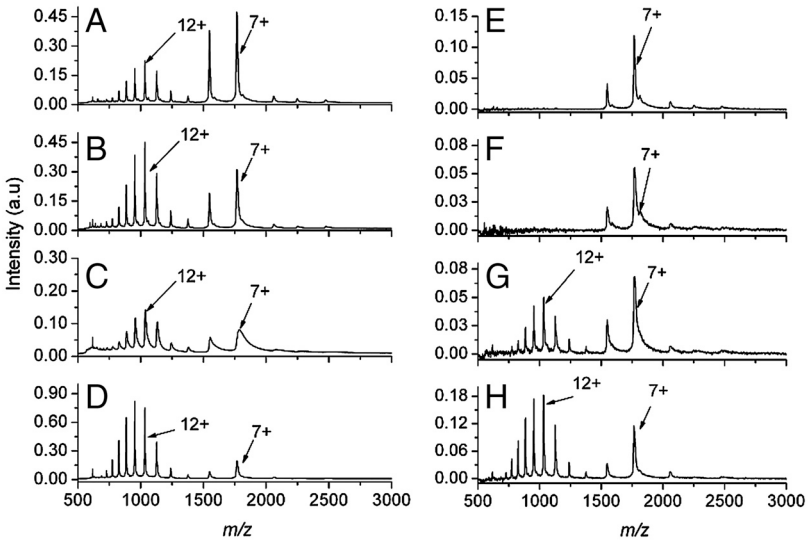

Fig. 1. Mass spectra of cytochrome c as a function of electrospray solvent pH. The conventional ESI mass spectra of cytochrome c measured at pH (*A*) 7.18, (*B*) 6.07, (*C*) 5.06, and (*D*) 4.06. The mass spectra resulting from the femtosecond laser-induced vaporization of aqueous cytochrome c (pH 7) followed by capture and ionization in the electrospray plume at pH (*E*) 7.18, (*F*) 6.07, (*G*) 5.06, and (*H*) 4.06.

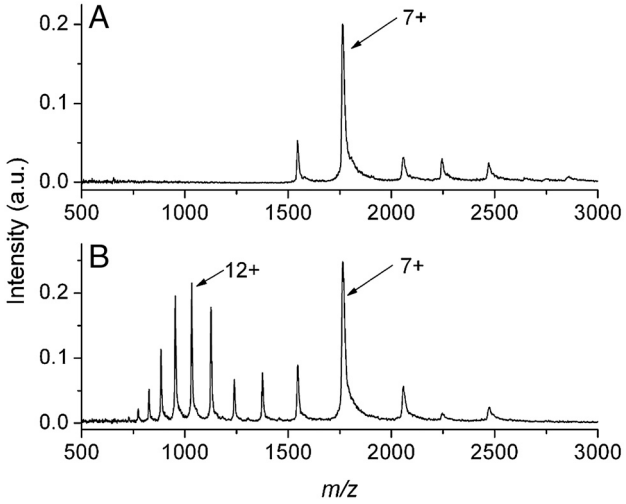

Fig. 2. Mass spectra of cytochrome c as a function of droplet pH. The mass spectra resulting from the nonresonant femtosecond laser-induced vaporization of aqueous cytochrome c dissolved in solution at pH 7 (*A*) and in solution at pH of approximately 3 (*B*) followed by capture and ionization in the electrospray plume at pH 7.06.

an unfolded conformation (37, 39), was also observed when the cytochrome c solution at pH 7 was electrosprayed. Unfolded cytochrome c is detected in the conventional ESI mass spectrum at neutral pH where only folded protein is expected because of denaturing in the electrospray solvent containing 50% methanol by volume (40, 41) and a decrease in pH in the electrospray droplet during the electrospray droplet formation process (42, 43).

The structural conformation of cytochrome c is sensitive to pH and should shift to higher charge states (with more states populated) as the pH decreases (41). As anticipated, the unfolded state of cytochrome c dominates the distribution under increasingly acidic solvent conditions (pH 6 to pH 4, Fig. 1 *B–D*). The conventional ESI-MS spectra obtained (Fig. 1 *A–D*) are in agreement with previous ESI-MS measurements as a function of pH (41).

When a femtosecond laser pulse interacts with a condensed phase system, electrons are excited resonantly via a single photon, or nonresonantly via multiphoton excitation. In either case, the energy of the nascent, "hot" electrons is transferred into the phonon modes of the system on the picosecond timescale (29, 44), a timescale which is many orders of magnitude shorter than that required for protein unfolding (45). If the protein is vaporized prior to achieving thermal equilibrium, the initial conformation may be maintained in the gas phase. The charge-state distribution of aqueous cytochrome c was analyzed to determine whether nonresonant femtosecond laser vaporization alters a protein's tertiary structure via thermal denaturation. The measured charge-state distributions (Fig. 1 *E–H*) resulting from the intense, nonresonant femtosecond laser vaporization with subsequent capture and ionization in an electrospray plume are quite different in comparison with conventional ESI-MS. Only the folded conformation (as revealed by the 8 and 7+ charge states) is detected when the vaporized protein was captured and ionized by an electrospray plume at pH 7.18 (Fig. 1*E*) or 6.07 (Fig. 1*F*). The data suggests that femtosecond laser vaporization prevents thermal denaturation preserving the condensed phase conformation of the protein upon transfer into the gas phase. In addition, intense, nonresonant femtosecond laser vaporization with electrospray postionization preserves the condensed phase conformation even when a denaturant (methanol) is present in the electrospray solvent. However, unfolded protein is observed in the mass spectrum when the vaporized protein is captured by an electrospray plume at pH 5.06 (Fig. 1*G*) and 4.06 (Fig. 1*H*), suggesting that the denaturation rate increases at higher acid concentrations in the electrospray plume.

To further explore the hypothesis that LEMS preserves the condensed phase conformation of the protein, we measured the charge-state distribution as a function of sample pH, specifically the pH of the protein solution subjected to laser vaporization. When cytochrome c is vaporized from a nondenaturing (pH 7) solution (46) and captured and ionized by a nondenaturing (pH 7) electrospray solvent, only folded protein is observed in the mass spectrum (Fig. 2*A*). The observation of the folded conformation is expected because the pH of both solvent systems (aqueous sample solution and the electrospray solvent) are nondenaturing. However, when cytochrome c is vaporized from a denaturing solution (pH ~3) with subsequent capture and ionization in a nondenaturing (pH 7) electrospray plume, unfolded pro-

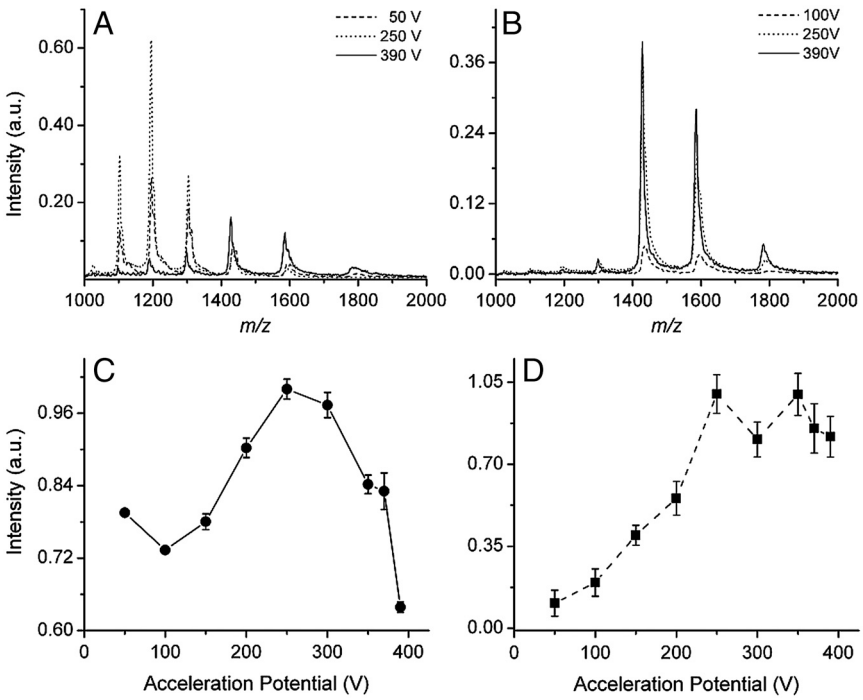

Fig. 3. Mass spectra and integrated signal intensities of lysozyme at different acceleration potentials. (*A*) The ESI mass spectra of lysozyme for the acceleration potentials of 50 V (dash), 250 V (dot), and 390 V (solid). (*B*) The LEMS mass spectra of lysozyme for the acceleration potentials of 100 V (dash), 250 V (dot), and 390 V (solid). The integrated ion signal intensity of lysozyme as a function of acceleration potential using (*C*) ESI-MS and (*D*) LEMS.

tein is observed in the mass spectrum (Fig. 2*B*). This observation reveals that the conformation of the condensed phase protein, folded or unfolded, is reflected in the ESI charge-state distribution and may be due to the vaporized protein's short interaction time with the electrospray plume. Nevertheless, these measurements further support the hypothesis that intense, nonresonant femtosecond laser vaporization of protein maintains the condensed phase conformation.

Quantification of Folded and Unfolded Protein in Conventional ESI-MS and LEMS. The ratio of folded cytochrome c to the total protein signal is plotted as a function of electrospray solvent pH for both techniques (Fig. 4) for the data shown in Fig. 1. At every pH measured, the fraction of folded protein is higher for the LEMS experiment in comparison to the conventional ESI-MS experiment. At pH 7.18 and 6.07, only folded protein is observed for the LEMS experiments whereas approximately 40% resides in the unfolded state for the ESI-MS experiments. The difference in the ratios is due to the protein spending minutes in solution allowing the folded/unfolded ratio to reach equilibrium at a given pH for the conventional ESI-MS experiments. In the LEMS experiment, the protein remains in the electrospray plume for approximately 100 ms, which is short compared to the timescale of several seconds required for unfolding to a denatured state (47). Therefore, the condensed phase conformation is detected in the mass spectrum because of the mismatch in these timescales. In addition, the detection of folded protein in the LEMS experiments could be partially due to the capture, solvation, and ionization of the vaporized sample by smaller droplets in the electrospray plume. Smaller droplets prevent a decrease in pH during the electrospray droplet formation process, reducing denaturation conditions in a manner similar to that seen in high gas flow ESI measurements (48, 49). However, as the pH decreases, the denaturation rate increases to a point that unfolding can occur during the short transit time spent in the electrospray solvent droplet prior to evaporation (50). Thus, a higher fraction of the protein is observed in the unfolded conformation. We conclude that the limited interaction time of the vaporized protein with the denaturing electrospray plume and the nonthermal vaporization mechanism enables LEMS to be a much softer mass spectrometric method than conventional ESI-MS.

CID of Aqueous Lysozyme in Conventional ESI-MS and LEMS. To test the hypothesis that LEMS transfers protein into the gas phase without conformational change, a second protein, hen egg white lysozyme, was investigated. The conventional ESI mass spectra of lysozyme at different acceleration potentials reveal that the observed charge-state distribution is highly sensitive to the collision energy (Fig. 3*A*). At an acceleration potential of 50 V, a bell-shaped distribution corresponding to the 13 to 8+ charge states is measured, suggesting that the protein is in an unfolded conformation (37, 41, 51). The bell-shaped distribution is maintained, but increases in intensity, as the acceleration potential approaches 250 V. The increase in signal intensity at higher acceleration potentials is attributed to the fact that the protein ions are moving at a higher velocity toward the skimmer. This higher velocity decreases the expansion of positive ions to regions outside of the skimmer inlet radius due to space charge (Coulomb repulsion) effects. In addition, the increase in ion abundance is also due to the removal of adducts (water and acetonitrile molecules) that are loosely bound to the lysozyme ion. The removal of these adducts transfers signal intensity from the adduct-bound lysozyme peak (e.g., $[M + 3H_2O + CH_3CN + nH^+]^{n+}$ indicated by the right shoulder on the n+ peaks) into the adduct-free lysozyme peak (n+, e.g., $[M + nH^+]^{n+}$). As the acceleration potential is further increased to 390 V, the ion signal decreases in intensity and shifts to lower charge states due to the collision-induced loss of loosely bound cations (e.g., H^+) (52, 53). The observed charge states correspond to an unfolded conformation of lysozyme with the disulfide bonds intact. If the disulfide bonds were reduced (broken), higher charge states, ranging from 20 to 12+, would be observed in the ESI mass spectrum (54).

The CID measurements are quantitatively different than those for conventional ESI-MS when an aliquot of lysozyme solution was vaporized using an intense, nonresonant femtosecond laser pulse, followed by capture and ionization in an electrospray plume. The LEMS mass spectrum for lysozyme collected at an acceleration potential of 100 V displays only the 10 and 9+ charge states corresponding to a folded conformation (Fig. 3*B*) (18, 55). Upon increasing the acceleration potential to 390 V, an increase in the ion intensity was observed with no additional fragmentation or change in the charge-state distribution. The increase in ion abundance at high acceleration potentials is attributed to the decrease in space charge effects and removal of loosely bound adducts, as seen with the conventional ESI-MS of lysozyme. The folded protein signal is dominant for the LEMS measurements in comparison to the conventional ESI-MS experiments at each collision energy, again suggesting that the folded structure (18) is preserved under the intense laser pulse conditions used for vaporization.

To further explore the hypothesis that intense, nonresonant femtosecond laser vaporization with electrospray postionization preserves the folded structure of proteins under conditions where conventional ESI-MS does not, the integrated ion signal from the various charge states as a function of collision energy for both techniques was measured. The total ion abundance contained in the conventional ESI mass spectra is plotted as a function of acceleration potential (Fig. 3*C*). As the acceleration potential increases to approximately 250 V, the lysozyme signal monotonically increases due to the reduction in space charge effects and

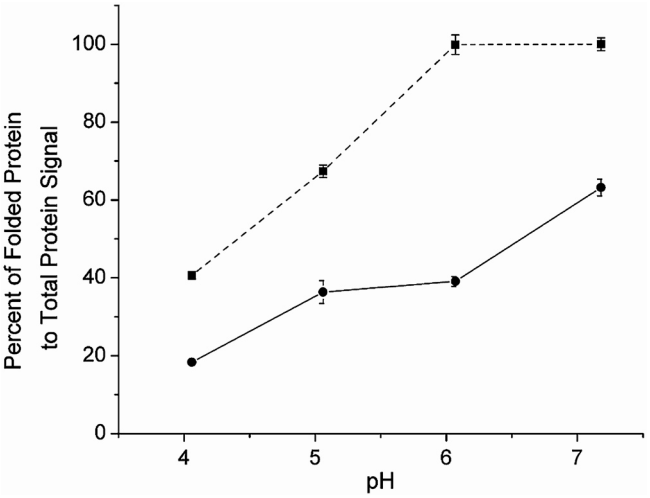

Fig. 4. Quantification of folded protein observed in the cytochrome c mass spectra. The percent of folded protein vs. the total protein signal resulting from the ESI-MS experiments (•, solid line) and the LEMS experiments (■, dashed line).

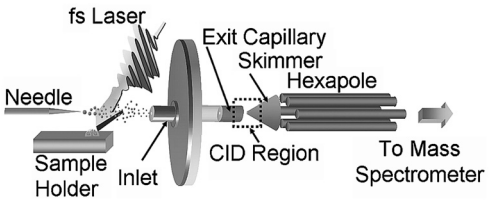

Fig. 5. Schematic of the LEMS apparatus. A nonresonant femtosecond laser irradiates an aqueous sample vaporizing the protein, which is captured and ionized by the electrospray plume prior to mass analysis, or CID with subsequent mass analysis.

loss of noncovalently bound adducts. However, above 250 V, a decrease in the intact ion signal intensity is measured due to charge reduction and fragmentation, which is consistent with the notion that a denatured protein has a larger CID cross section.

In the case of femtosecond laser-induced vaporization with electrospray postionization, the integrated ion signal as a function of acceleration potential reveals no evidence for fragmentation at higher collision energy (Fig. 3*D*). The lack of fragmentation and the absence of charge reduction is consistent with vaporization of folded protein. There is no decrease in signal above an acceleration potential of 250 V because the folded structure suffers fewer collisions. Any energy deposited during the collision is rapidly transferred away from the impact site due to the folded conformation providing multiple points of contact, facilitating intramolecular energy redistribution. Therefore, we conclude that the structure of the gas phase lysozyme is quite different for the conventional ESI-MS experiments and the LEMS experiments.

The nonresonant femtosecond laser pulse has sufficient intensity (10^{13} W/cm^2) to couple into pure protein (13), water and/or the metal substrate via a multiphonon excitation to enable the transfer of sample into the gas phase. The vaporization process resulting from the absorption of the laser pulse energy may proceed through several possible mechanisms. In one such mechanism, the condensed phase system can be excited into a repulsive adsorbate-substrate or a repulsive adsorbate-adsorbate (e.g., protein-protein, protein-water) electronic state by either the direct absorption of photons or by collisions with hot electrons (1–10 eV) (56–58). This excitation converts photon energy into potential energy, which is subsequently transformed into translational kinetic energy due to electronic repulsion, enabling the transfer of molecules and clusters into the gas phase.

In addition, it is also possible that the electrons created at the metal surface can undergo cooling via collisions leading to the direct vibrational excitation of intramolecular bonds of the molecules (59). The excitation of the vibrational modes leads to expansion of the molecules against neighboring molecules, or the substrate, leading to the creation of a pressure pulse ejecting molecules and clusters from the surface. The temperature of the vaporized material is equal to that of the local surface (60).

Once vaporized, the molecules or clusters undergo expansion into the gas phase where collisions with the background gas further decrease the internal energy, lowering the temperature and preventing molecular dissociation and unfolding of the protein (61, 62). We estimate that the final temperature of the molecules prior to capture in the electrospray plume is approximately 300 K. This excitation mechanism allows the detection of intact protein, preserving the condensed phase conformation, when nonresonant, femtosecond laser vaporization is combined with electrospray postionization and time-of-flight mass analysis.

Concluding Remarks

An intense, (10^{13} W/cm^2) nonresonant femtosecond laser pulse can be used to vaporize macromolecules from their native environment into the gas phase for capture and ionization in an electrospray plume at atmospheric pressure. The discovery that intact vaporization of condensed phase protein can be induced using a nonresonant femtosecond laser pulse (13, 30–34) was unanticipated because isolated protein in the gas phase under vacuum conditions will inevitably ionize and fragment (35, 36). The ability to analyze the molecular weight of proteins using LEMS was recently reported (13) and here we have shown that a protein's structural conformation is preserved upon intense, nonresonant femtosecond laser vaporization. The ultrafast deposition of energy into the sample results in the nonthermal transfer of adsorbed protein into the gas phase preventing thermal denaturation (i.e., alteration of protein's conformation). In addition to the nonthermal vaporization mechanism, the limited interaction time of the vaporized protein with the denaturing solvent enables LEMS to be a softer vaporization/ionization method than conventional ESI-MS when using identical electrospray conditions. The ability to vaporize proteins while maintaining a folded conformation is an important step toward the measurement of noncovalent protein-protein and enzyme-substrate interactions. These measurements suggest that investigation of the ex vivo protein conformation analysis is now possible.

Materials and Methods

Sample Preparation. A solid sample of horse heart cytochrome c was purchased from Sigma Aldrich and used without purification. For the conventional ESI-MS of cytochrome c, a 2×10^{-4} M stock solution was prepared in deionized (DI) water containing 10 mM ammonium acetate. A 1×10^{-5} M solution was prepared by diluting an aliquot of the stock solution in pH adjusted 1:1 (vol:vol) methanol:water solution containing 5 mM ammonium acetate (pH range 7–4). A 8×10^{-4} M cyctochrome c solution was prepared in DI water (pH 7), to obtain the folded conformation (46) for LEMS analysis. A denatured cytochrome c sample was also prepared for LEMS analysis by diluting a portion of the 8×10^{-4} M cytochrome c solution in a 1:1 (vol:vol) ratio with 1:1 (vol:vol) methanol:water containing 5 mM ammonium acetate (pH 4). This solution was further acidified with acetic acid to a pH of approximately 3.

A solid sample of hen egg white lysozyme was purchased from Sigma Aldrich and used without purification. For the conventional ESI-MS analysis of lysozyme, a 1×10^{-4} M solution was prepared in 1:1 (vol:vol) acetonitrile:water with 1% acetic acid (pH 3.25). For the LEMS analysis, a 1×10^{-3} M solution of lysozyme was prepared in DI water.

Laser Vaporization and Ionization Apparatus. A regenerative amplifier created an 800 nm, 75 fs, 2.5 mJ laser pulse at 10 Hz, which was attenuated to 1.5 mJ/pulse prior to being focused to a spot size of approximately 250 μm in diameter, using a 16.9-cm focal length lens. The laser pulse had an incident angle of 45° with respect to the aqueous sample (a 10 μL aliquot) deposited on a steel substrate. The aqueous sample was vaporized allowing for capture and ionization by an electrospray plume composed of pH adjusted 5 mM ammonium acetate buffer in 1:1 (vol:vol) methanol:water (cytochrome c experiments) or 1:1 (vol:vol) acetonitrile:water acidified with 1% glacial acetic acid (lysozyme experiments) traveling perpendicular to the laser-vaporized material (Fig. 5). The flow rate of the electrospray solvent was 3 μL/min as set by a syringe pump. The charged droplets, containing the captured analyte, were dried by counter propagating nitrogen gas at 180 °C prior to entering the inlet capillary.

Mass Spectrometry. An electrospray source ionizes and transfers sample into a vacuum chamber where pulsed deflection orthogonal time-of-flight mass analysis is performed (Fig. 5). The positive ions are subsequently detected and the resulting mass spectra were averaged for 5 s totaling 50 mass spectra (50 laser shots) for LEMS analysis (20 s for conventional ESI-MS measurements). For the conventional ESI-MS measurements reported here, the solution was electrosprayed at a flow rate of 0.6 μL/min and no laser was present at the time of analysis. The electrosprayed solutions were composed of the same solvent as that used for LEMS analysis of the respective protein samples. The ESI experiments had the same voltage conditions as the LEMS experiments, to ensure identical conditions for all experiments.

CID Experiments. A large number of protein-N_2 collisions occur in the region between the electrospray capillary exit and the skimmer in the ESI source, which is maintained at a relatively high pressure, approximately 1.2 Torr (Fig. 5). The maximum energy imparted into the internal modes of the protein upon collision with N_2 scales with the magnitude of the acceleration potential, which can be adjusted by varying the voltage difference between the capillary exit and the skimmer in the electrospray source. Fifty mass spectra were acquired and averaged at each acceleration potential for both the conventional ESI-MS and LEMS experiments.

ACKNOWLEDGMENTS. We thank Laine Radell and Kuriakose Simon for their help with data collection and the National Science Foundation (CHE0518497 and CHE0957694) for their financial support.

1. Mohideen U, et al. (1993) High-intensity above-threshold ionization of He. *Phys Rev Lett* 71:509–512.
2. Freeman RR, et al. (1987) Above-threshold ionization with subpicosecond laser-pulses. *Phys Rev Lett* 59:1092–1095.
3. Brabec T, Krausz F (2000) Intense few-cycle laser fields: Frontiers of nonlinear optics. *Rev Mod Phys* 72:545–591.
4. Popmintchev T, et al. (2009) Phase matching of high harmonic generation in the soft and hard X-ray regions of the spectrum. *Proc Natl Acad Sci USA* 106:10516–10521.
5. Mauritsson J, et al. (2006) Attosecond pulse trains generated using two color laser fields. *Phys Rev Lett* 97:013001.
6. Codling K, Frasinski LJ (1993) Dissociative ionization of small molecules in intense laser fields. *J Phys B At Mol Opt Phys* 26:783–809.
7. Lezius M, et al. (2001) Nonadiabatic multielectron dynamics in strong field molecular ionization. *Phys Rev Lett* 86:51–54.
8. Markevitch AN, et al. (2003) Nonadiabatic dynamics of polyatomic molecules and ions in strong laser fields. *Phys Rev A* 68:011402.
9. Ledingham KWD, McKenna P, Singhal RP (2003) Applications for nuclear phenomena generated by ultra-intense lasers. *Science* 300:1107–1111.
10. Ditmire T, et al. (1999) Nuclear fusion from explosions of femtosecond laser-heated deuterium clusters. *Nature* 398:489–492.
11. Worner HJ, Niikura H, Bertrand JB, Corkum PB, Villeneuve DM (2009) Observation of electronic structure minima in high-harmonic generation. *Phys Rev Lett* 102:103901.
12. Nugent-Glandorf L, Scheer M, Samuels DA, Bierbaum V, Leone SR (2002) A laser-based instrument for the study of ultrafast chemical dynamics by soft X-ray-probe photoelectron spectroscopy. *Rev Sci Instrum* 73:1875–1886.
13. Judge EJ, Brady JJ, Levis RJ (2010) Mass analysis of biological macromolecules at atmospheric pressure using nonresonant femtosecond laser vaporization and electrospray ionization. *Anal Chem* 82:10203–10207.
14. Palczewski K, et al. (2000) Crystal structure of rhodopsin: A G protein-coupled receptor. *Science* 289:739–745.
15. Tjandra N, Bax A (1997) Direct measurement of distances and angles in biomolecules by NMR in a dilute liquid crystalline medium. *Science* 278:1111–1114.
16. Tullius TD, Dombroski BA (1986) Hydroxyl radical "footprinting": High-resolution information about DNA-protein contacts and application to lambda repressor and Cro protein. *Proc Natl Acad Sci USA* 83:5469–5473.
17. Fenn JB, Mann M, Meng CK, Wong SF, Whitehouse CM (1989) Electrospray ionization for mass spectrometry of large biomolecules. *Science* 246:64–71.
18. Grandori R (2003) Origin of the conformation dependence of protein charge-state distributions in electrospray ionization mass spectrometry. *J Mass Spectrom* 38:11–15.
19. Seeley EH, Oppenheimer SR, Mi D, Chaurand P, Caprioli RM (2008) Enhancement of protein sensitivity for MALDI imaging mass spectrometry after chemical treatment of tissue sections. *J Am Soc Mass Spectrom* 19:1069–1077.
20. Dreisewerd K, Schürenberg M, Karas M, Hillenkamp F (1995) Influence of the laser intensity and spot size on the desorption of molecules and ions in matrix-assisted laser desorption/ionization with a uniform beam profile. *Int J Mass Spectrom* 141:127–148.
21. Figueroa ID, Russell DH (1999) Matrix-assisted laser desorption ionization hydrogen/deuterium exchange studies to probe peptide conformational changes. *J Am Soc Mass Spectrom* 10:719–731.
22. Santrucek J, Strohalm M, Kadlcík V, Hynek R, Kodícek M (2004) Tyrosine residues modification studied by MALDI-TOF mass spectrometry. *Biochem Biophys Res Commun* 323:1151–1156.
23. Wales TE, Engen JR (2006) Hydrogen exchange mass spectrometry for the analysis of protein dynamics. *Mass Spectrom Rev* 25:158–170.
24. Nemes P, Vertes A (2007) Laser ablation electrospray ionization for atmospheric pressure, in vivo, and imaging mass spectrometry. *Anal Chem* 79:8098–8106.
25. Huang M-Z, Jhang S-S, Cheng C-N, Cheng S-C, Shiea J (2010) Effects of matrix, electrospray solution, and laser light on the desorption and ionization mechanisms in electrospray-assisted laser desorption ionization mass spectrometry. *Analyst* 135:759–766.
26. Sampson JS, Muddiman DC (2009) Atmospheric pressure infrared (10.6 μm) laser desorption electrospray ionization (IR-LDESI) coupled to a LTQ Fourier transform ion cyclotron resonance mass spectrometer. *Rapid Commun Mass Spectrom* 23:1989–1992.
27. Sampson JS, Murray KK, Muddiman DC (2009) Intact and top-down characterization of biomolecules and direct analysis using infrared matrix-assisted laser desorption electrospray ionization coupled to FT-ICR mass spectrometry. *J Am Soc Mass Spectrom* 20:667–673.
28. Rezenom YH, Dong J, Murray KK (2008) Infrared laser-assisted desorption electrospray ionization mass spectrometry. *Analyst* 133:226–232.
29. Elsayed-Ali HE, Norris TB, Pessot MA, Mourou GA (1987) Time-resolved observation of electron-phonon relaxation in copper. *Phys Rev Lett* 58:1212–1215.
30. Brady JJ, Judge EJ, Levis RJ (2010) Identification of explosives and explosive formulations using laser electrospray mass spectrometry. *Rapid Commun Mass Spectrom* 24:1659–1664.
31. Judge EJ, Brady JJ, Barbano PE, Levis RJ (2011) Nonresonant femtosecond laser vaporization with electrospray post-ionization for ex vivo plant tissue typing using compressive linear classification. *Anal Chem* 83:2145–2151.
32. Brady JJ, Judge EJ, Levis RJ (2011) Analysis of amphiphilic lipids and hydrophobic proteins using nonresonant femtosecond laser vaporization with electrospray post-ionization. *J Am Soc Mass Spectrom* 22:762–772.
33. Judge EJ, Brady JJ, Levis RJ (2010) Mass analysis of pharmaceutical compounds from glass, cloth, steel and wood surfaces at atmospheric pressure using non-resonant femtosecond laser vaporization and electrospray ionization. *Anal Chem* 82:3231–3238.
34. Brady JJ, Judge EJ, Levis RJ (2009) Mass spectrometry of intact neutral macromolecules using intense non-resonant femtosecond laser vaporization with electrospray post-ionization. *Rapid Commun Mass Spectrom* 23:3151–3157.
35. Levis RJ, DeWitt MJ (1999) Photoexcitation, ionization, and dissociation of molecules using intense near-infrared radiation of femtosecond duration. *J Phys Chem A* 103:6493–6507.
36. Weinkauf R, Aicher P, Wesley G, Grotemeyer J, Schlag EW (1994) Femtosecond versus nanosecond multiphoton ionization and dissociation of large molecules. *J Phys Chem* 98:8381–8391.
37. Fligge TA, Kast J, Bruns K, Przybylski M (1999) Direct monitoring of protein-chemical reactions utilizing nanoelectrospray mass spectrometry. *J Am Soc Mass Spectrom* 10:112–118.
38. Clemmer DE, Hudgins RR, Jarrold MF (1995) Naked protein conformations: Cytochrome c in the gas phase. *J Am Chem Soc* 117:10141–10142.
39. Valentine SJ, Clemmer DE (1997) H/D exchange levels of shape-resolved cytochrome c conformers in the gas phase. *J Am Chem Soc* 119:3558–3566.
40. Drew HR, Dickerson RE (1978) The unfolding of the cytochromes c in methanol and acid. *J Biol Chem* 253:8420–8427.
41. Konermann L, Douglas DJ (1997) Acid-induced unfolding of cytochrome c at different methanol concentrations: Electrospray ionization mass spectrometry specifically monitors changes in the tertiary structure. *Biochemistry* 36:12296–12302.
42. Nemes P, Goyal S, Vertes A (2008) Conformational and noncovalent complexation changes in proteins during electrospray ionization. *Anal Chem* 80:387–395.
43. Van Berkel GJ, Zhou F, Aronson JT (1997) Changes in bulk solution pH caused by the inherent controlled-current electrolytic process of an electrospray ion source. *Int J Mass Spectrom* 162:55–67.
44. Levis RJ (1994) Laser desorption and ejection of biomolecules from the condensed phase into the gas phase. *Annu Rev Phys Chem* 45:483–518.
45. Williams S, et al. (1996) Fast events in protein folding: Helix melting and formation in a small peptide. *Biochemistry* 35:691–697.
46. Wood TD, et al. (1995) Gas-phase folding and unfolding of cytochrome c cations. *Proc Natl Acad Sci USA* 92:2451–2454.
47. Ikai A, Fish WW, Tanford C (1973) Kinetics of unfolding and refolding of proteins: II. Results for cytochrome c. *J Mol Biol* 73:165–184.
48. Takats Z, Wiseman JM, Gologan B, Cooks RG (2004) Electrosonic spray ionization. A gentle technique for generating folded proteins and protein complexes in the gas phase and for studying ion–molecule reactions at atmospheric pressure. *Anal Chem* 76:4050–4058.
49. Yang P, Cooks RG, Ouyang Z, Hawkridge AM, Muddiman DC (2005) Gentle protein ionization assisted by high-velocity gas flow. *Anal Chem* 77:6174–6183.
50. Peng IX, Loo RRO, Shiea J, Loo JA (2008) Reactive-electrospray-assisted laser desorption/ionization for characterization of peptides and proteins. *Anal Chem* 80:6995–7003.
51. Mirza UA, Cohen SL, Chait BT (1993) Heat-induced conformational changes in proteins studied by electrospray ionization mass spectrometry. *Anal Chem* 65:1–6.
52. Rogers DA, Ray SJ, Hieftje GM (2010) An electrospray/inductively coupled plasma dual-source time-of-flight mass spectrometer for rapid metallomic and speciation analysis Part 1. Molecular channel characterization. *Metallomics* 2:271–279.
53. Cole RB (2000) Some tenets pertaining to electrospray ionization mass spectrometry. *J Mass Spectrom* 35:763–772.
54. Loo JA, Edmonds CG, Udseth HR, Smith RD (1990) Effect of reducing disulfide-containing proteins on electrospray ionization mass spectra. *Anal Chem* 62:693–698.
55. Fenn JB (1993) Ion formation from charged droplets: Roles of geometry, energy, and time. *J Am Soc Mass Spectrom* 4:524–535.
56. Arnolds H, Rehbein CEM, Roberts G, Levis RJ, King DA (1999) Femtosecond near-infrared laser desorption of multilayer benzene on Pt{111}: Spatial origin of hyperthermal desorption. *Chem Phys Lett* 314:389–395.
57. Arnolds H, Levis RJ, King DA (2003) Vibrationally assisted DIET through transient temperature rise: The case of benzene on Pt{111}. *Chem Phys Lett* 380:444–450.
58. Arnolds H, Rehbein C, Roberts G, Levis RJ, King DA (2000) Femtosecond near-infrared laser desorption of multilayer benzene on Pt{111}: A molecular Newton's cradle? *J Phys Chem B* 104:3375–3382.
59. Williams P, Sundqvist B (1987) Mechanism of sputtering of large biomolecular ions by impact of highly ionizing particles. *Phys Rev Lett* 58:1031–1034.
60. Johnson RE, Sundqvist BUR, Ens W (1991) Laser-pulse ejection of organic molecules from a matrix: Lessons from fast-ion-induced ejection. *Rapid Commun Mass Spectrom* 5:574–578.
61. Schieltz DM, et al. (1992) Mass spectrometry of DNA mixtures by laser ablation from frozen aqueous solution. *Rapid Commun Mass Spectrom* 6:631–636.
62. Nelson RW, Thomas RM, Williams P (1990) Time-of-flight mass spectrometry of nucleic acids by laser ablation and ionization from a frozen aqueous matrix. *Rapid Commun Mass Spectrom* 4:348–351.